JOURNAL OF MATERIALS SCIENCE 30 (1995) 898–903

Corrosion behaviour of aluminium matrix composites

G. W. ROPER, P. A. ATTWOOD
Shell Research Limited, Thornton Research Centre, P. O. Box 1, Chester CH1 3SH

Samples of aluminium alloy 2014 reinforced with 20–40 vol % of alumina or silicon carbide particles were tested by the potentiodynamic polarization technique. The chosen medium was 0.1M lithium perchlorate which tends to cause localized corrosion. The measurements revealed no impairment of the corrosion performance of the matrix alloy as a result of the presence of the reinforcement phase.

1. Introduction

Particulate reinforcement of a metal is aimed primarily at influencing the mechanical properties of the resulting composite. However, it is important that other properties are not impaired and one of these is corrosion behaviour. To investigate this, a number of composite samples were obtained from Atomic Energy Authority (AEA) Technology, Harwell based on the aluminium alloy 2014, having the nominal composition 4.4% Cu, 0.8% Mn, 0.8% Si, 0.4% Mg, bal. Al.

One of the samples was the original unreinforced alloy, while the remainder formed two series of metal matrix composites. Reinforcement in the first of these comprised respectively: 20, 30 and 40% by volume of alumina particles. A section through the 30 vol% reinforced sample is shown in plate 1. The particles were spherical and approximately 10 μm in diameter. Silicon carbide particles were the reinforcement in the second series of samples, again containing 20, 30 and 40 vol% of particles. Plate 2 shows a section through the 30 vol% reinforced sample; these particles were of a similar size to the alumina particles, but more angular in shape. All the samples were prepared by rolling of vacuum hot pressed powder mixtures, followed by a 500 °C anneal and air cool. The unreinforced sample was further given a T6 heat treatment, i.e. solution heat treated and artificially aged.

2. Potentiodynamic polarization test method

When a metal specimen is immersed in an electrolyte, both oxidation and reduction reactions may occur at its surface. Generally it is the metal that oxidizes, while a constituent of the electrolyte is reduced. The specimen adopts a so-called 'rest potential' or 'corrosion potential', denoted by E_{corr}. At E_{corr} the anodic and cathodic currents are equal in magnitude, i.e. the rate of oxidation is equal to the rate of reduction.

If a specimen is forced by some external means to adopt a potential other than its rest potential, electrical equilibrium is disturbed. For example, a more positive potential causes the anodic current to exceed the cathodic current; hence a net, measurable current will flow. This is the principle underlying the potentiodynamic polarization test method. The specimen, which acts as the working electrode, is placed in a corrosion cell together with counter and reference electrodes, as illustrated in Fig. 1. The three electrodes are connected to a potentiostat. The potential of the specimen with respect to a suitable reference electrode

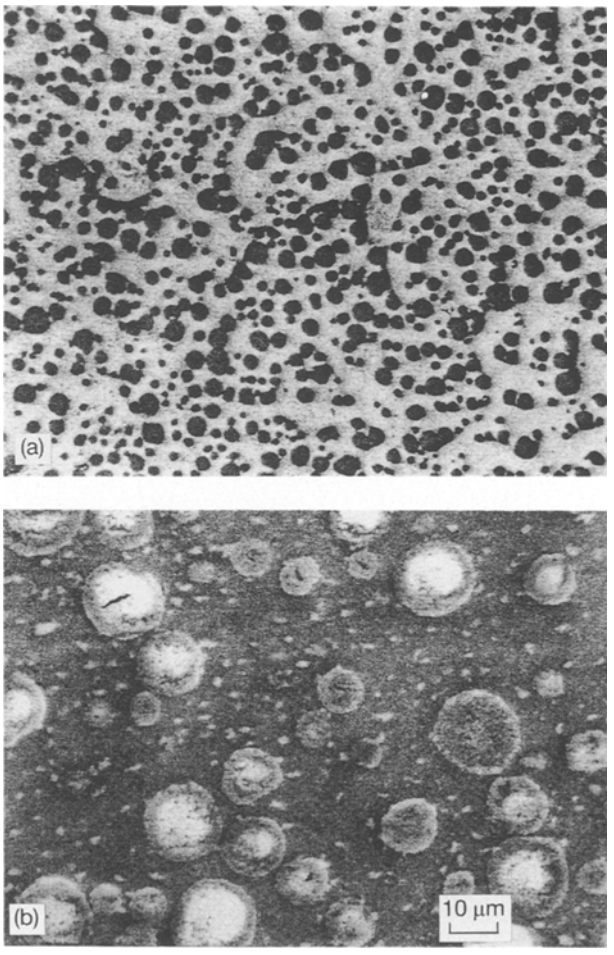

Plate 1 Section through 30 vol% alumina reinforced composite. (a) Optical micrograph (× 200). (b) Electron micrograph (× 1000).

0022–2461

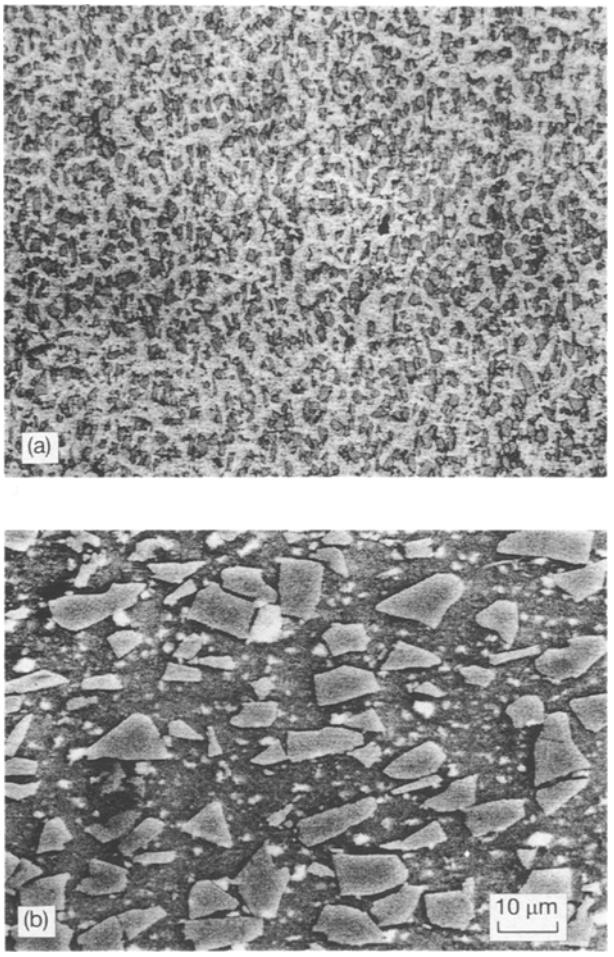

Plate 2 Section through 30 vol% SiC reinforced composite. (a) Optical micrograph (×200). (b) Electron micrograph (×1000).

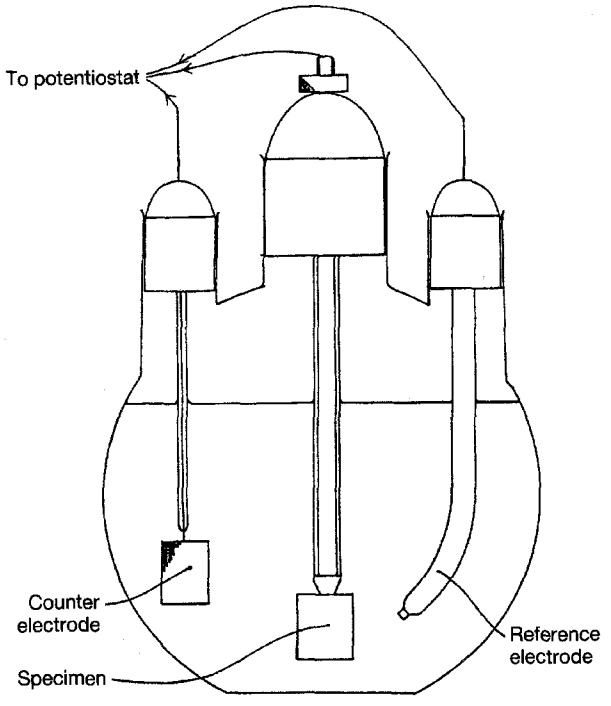

Figure 1 The corrosion cell.

is controlled by the potentiostat while the current between the specimen and the noble metal counter electrode is measured. The logarithm of this current is plotted versus the applied potential to obtain the characteristic potentiodynamic polarization plot.

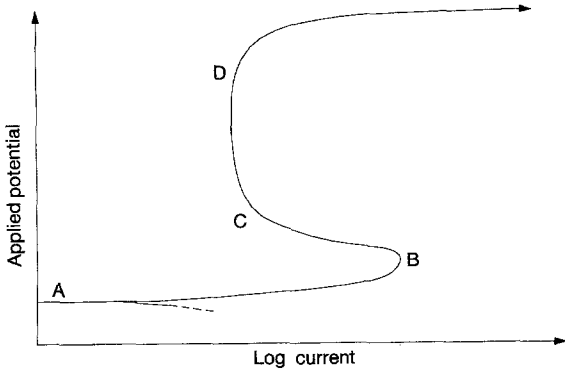

Figure 2 Theoretical potentiodynamic polarization plot.

An idealized plot for a metal displaying active/passive characteristics, is shown in Fig. 2. Point A is the rest potential where no net external current flows; (although strictly, of course, the point of zero current does not appear on a graph with a log scale). As the applied potential is made more positive (region A–B), the net current and hence also the corrosion rate increase. At Point B, increasing the potential further no longer results in an increased current. In fact, from B to C the current decreases with increasing applied potential. This loss of chemical reactivity is a result of the formation of a passive film on the surface of the specimen. In the potential range from C to D, the current remains constant; the specimen is said to be passivated. With a further increase in potential, the potential of the O_2/OH^- half cell can be reached and oxygen is liberated as illustrated by the increase in current beyond Point D. In certain electrolytes, e.g. those containing halide ions, a slightly different potentiodynamic profile can be obtained. As the potential is increased in the region C–D halide ions can be strongly adsorbed and this condition can lead to localized breakdown of the passive film. The resultant localized or pitting corrosion is evidenced by an increase in the current. The potential at which this sudden increase in current is observed following pit initiation is referred to as the critical pitting potential (E_{pit}).

Critical pitting potentials have been used for many years to predict the susceptibility of materials to undergo localized attack. Wilde [1] amongst others, has suggested that favourable correlations between long term corrosion behaviour and electrochemical polarization testing may also be obtained by measuring the area of the hysteresis loop obtained from cyclic polarization measurements.

The actual shape of the plot obtained experimentally depends on the form and intersection of the individual anodic and cathodic polarization curves. Figs 3(a), (c) and (e) show a theoretical anodic polarization curve, upon each of which is superimposed a different theoretical cathodic curve, such as the one for hydrogen evolution. The point (or points) at which these two curves intersect is E_{corr}, since the net current is zero at this point.

If the cathodic curve intersects the anodic curve in the passive region, as in Fig. 3(e), then the material passivates spontaneously. The experimentally obtained curve is derived from the separate anodic and cathodic curves and is illustrated in Fig 3(f). No active

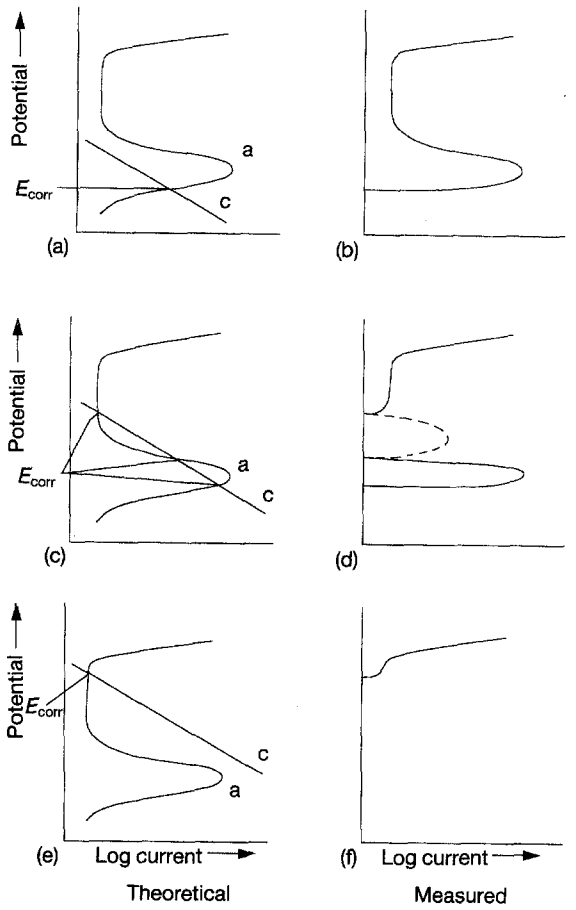

Figure 3 Three different cases of theoretical and actual potentiodynamic polarization plots. (a), (c) and (e). Three possible combinations of anodic, (a) and cathodic, (c) polarization curves. (b), (d) and (f) corresponding combined polarization curves as measured by the potentiodynamic technique.

to passive transition occurs in this case, since the material is passive at its rest potential.

Alternatively, if the cathodic curve intersects the anodic curve in the active region, as shown in Fig. 3(a), then the specimen will be active at its rest potential. The resultant experimental plot, Fig. 3(b), shows a characteristic active to passive transition.

A third possibility is for the cathodic curve to intersect the anodic curve at three places, as illustrated in Fig. 3(c). In this case there are three possible rest potentials and the resultant plot, Fig. 3(d), can show multiple loops, where the specimen is anodic of one rest potential but cathodic of another.

Potentiodynamic polarization plots thus give a qualitative 'finger-print' of the corrosion behaviour of a metal in a given environment and can be used to show any differences in electrochemical behaviour between various metal/environment systems. Of the three situations depicted in Fig. 3, the one illustrated by Figs 3(e) and (f) is the most desirable in a real system. since the metal is naturally passivated.

3. Experimental procedure and results

3.1. Apparatus

The potentiodynamic polarization curves for each of the test specimens were recorded using a PAR model 173 Potentiostat/Galvanostat coupled to a PAR model 175 Universal Programmer. Although the geometric areas of the specimens under evaluation were similar, there were variations in electroactive areas owing to the presence of the inert second phase. However, it was difficult to quantify this effect precisely and so, since small variations in current are not significant on a log scale, no attempt was made to normalize corrosion currents for surface area in this study. The polarization curves were displayed on a Bryans 26000 X–Y recorder. A conventional three arm corrosion test cell (Fig. 1) containing a platinum gauze counter electrode and standard calomel reference electrode was used throughout this work.

Specimens of approximately $20 \times 20 \times 5$ mm were cut from each of the samples supplied and mounted on the threaded specimen holder. The various areas of exposed metal (with the exception of the specimen itself) were then coated with silicone rubber to prevent galvanic effects. The specimens were surface ground on successively finer wet and dry papers to an ultimate finish of 1000 grit. This was to remove the surface layer thought to be contaminated with copper by the rolling operation and also to ensure that all specimens had the same surface finish for testing.

3.2. Procedure

An aerated 1 M aqueous solution of sodium chloride was initially chosen as the test environment. Once each specimen was placed into the corrosion cell, the rest potential was allowed to stabilize over a period of between one and two hours. The polarization sweep was then started from 20 mV cathodic of the rest potential and scanned in an anodic direction up to the potential at which a current of 100 mA was recorded. The sweep rate was set at 0.1 mV sec^{-1}.

Potentiodynamic sweeps were carried out on an unreinforced specimen and a specimen of the 40 vol% alumina composite; the plots are shown in Figs 4 and 5 respectively. There was very little passive behaviour before the onset of pitting, for either specimen. For comparison, the potentiodynamic sweep for pure aluminium exposed to the same chloride-containing environment was also obtained. The resulting plot

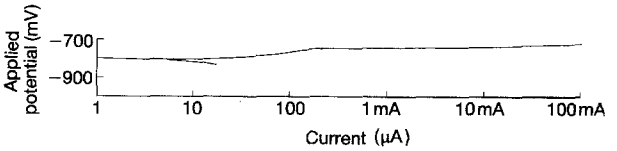

Figure 4 Unreinforced 2014 Al alloy in 1 M sodium chloride.

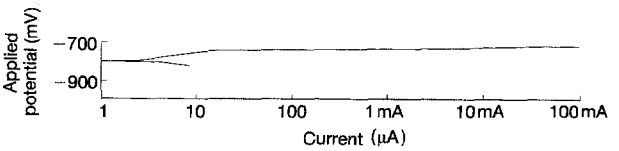

Figure 5 2014 Al + 40% vol% alumina specimen in 1 M sodium chloride.

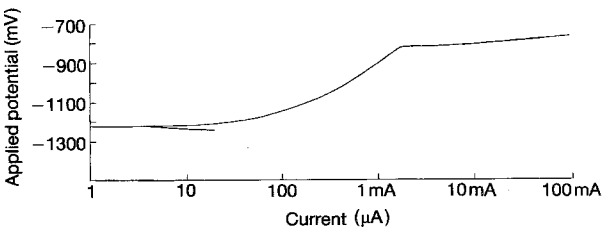

Figure 6 Pure aluminium specimen in 1 M sodium chloride.

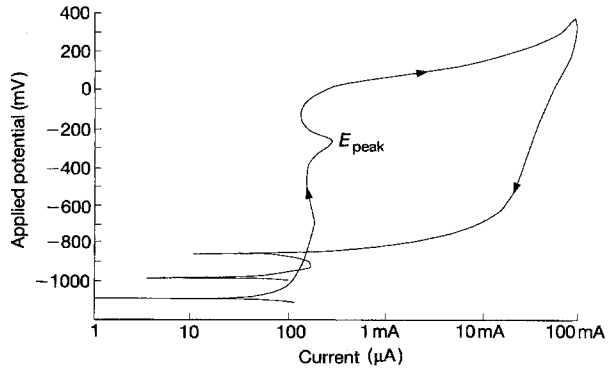

Figure 7 Unreinforced 2014 A1 alloy in 0.1 M lithium perchlorate.

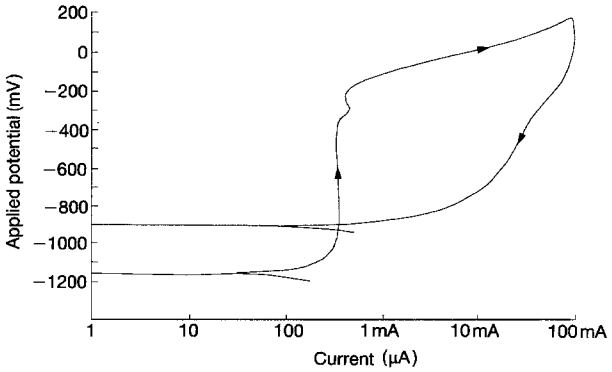

Figure 8 2014 A1 + 40 vol% alumina specimen in 0.1 M lithium perchlorate.

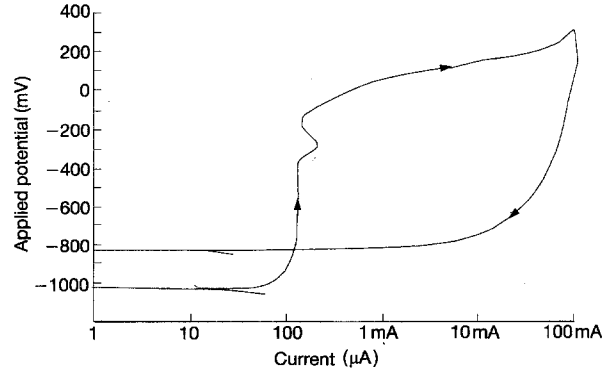

Figure 9 2014 A1 + 40 vol% SiC specimen in 0.1 M lithium perchlorate.

(Fig. 6) revealed a passive range of 400 mV before pitting occurred. This was greater than the 50 mV range seen for the 2014 aluminium alloy, principally because of the lower rest potential of pure aluminium.

Since there were only slight differences between the anodic sweeps recorded for the most heavily reinforced specimen and the matrix alloy itself, it was decided to continue the corrosion testing in a less aggressive environment. A 0.1 M lithium perchlorate solution was selected as the test environment. The perchlorate ion is a symmetric low charge density ion and so its complexing power and its tendency to adsorb on the electrode surface are considerably less than those of Cl^{-2}. Consequently, this electrolyte has less of a tendency to induce breakdown of the protective surface film and so the passive region is often extended over a much broader potential range. This would enable differences in the electrochemical corrosion properties of the matrix alloy and the reinforced specimens to be more readily distinguished.

The experimental procedure adopted using 0.1 M solutions of lithium perchlorate was similar to that used previously, except that the solutions were deaerated using high purity argon and the potential scan direction was reversed when a current of 100 mA was reached to provide a measure of the repassivation hysteresis.

Figs 7, 8 and 9 show examples of the potentiodynamic polarization plots obtained with the lithium

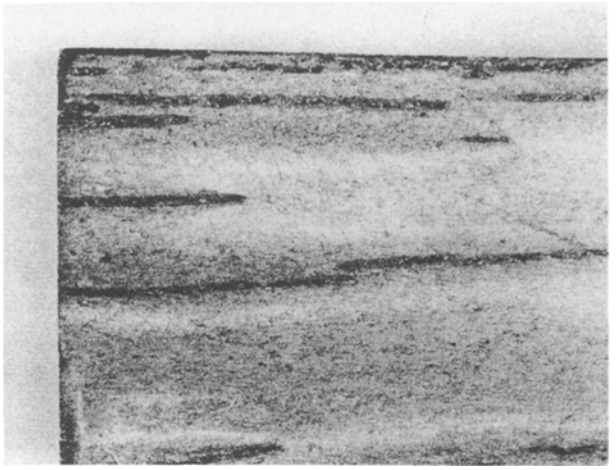

Plate 3 Unreinforced 2014 Al alloy specimen after potentiodynamic sweep (× 8).

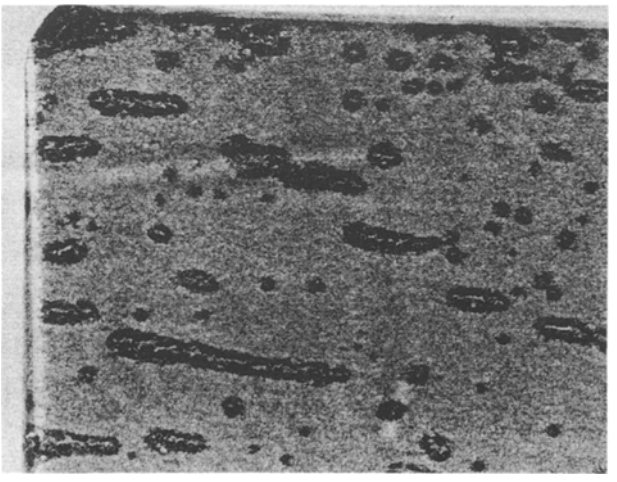

Plate 4 40 vol% alumina reinforced specimen after potentiodynamic sweep (× 8).

TABLE I Potentiodynamic polarization plot data using the 0.1 M lithium perchlorate solution and specimen surface area values.

Specimen material	Surface area (cm^2)	E_{corr} (V)	E_{pit}[a] (V)	E_{peak}[b] (V)
2014 Alloy	11.7	− 1.089	− 0.120	− 0.270
2014 Alloy + 20 vol % Al_2O_3	9.9	− 1.041	+ 0.090	− 0.290
2014 Alloy + 30 vol % Al_2O_3	11.5	− 1.022	− 0.080	− 0.260
2014 Alloy + 40 vol % Al_2O_3	14.7	− 1.152	− 0.210	− 0.280
2014 Alloy + 20 vol % SiC	12.5	− 1.022	+ 0.060	− 0.250
2014 Alloy + 30 vol % SiC	13.2	− 1.003	− 0.210	− 0.280
2014 Alloy + 40 vol % SiC	10.2	− 1.027	− 0.170	− 0.270
Pure aluminium	14.5	− 1.657	− 0.010	None

[a] Critical pitting potential
[b] Potential of peak in passive region (see for example Fig. 7)

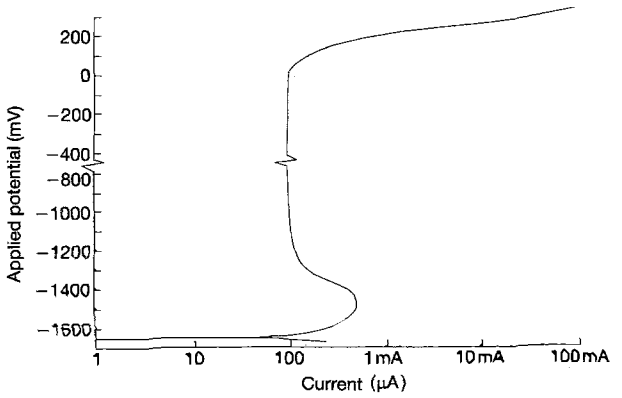

Figure 10 Pure aluminium specimen in 0.1 M lithium perchlorate.

perchlorate test solution. As anticipated, this solution permitted testing over a far greater potential range before the onset of pitting. The data obtained from the plots are summarized in Table I and photographs of specimens after the tests, showing pits, are illustrated in Plates 3 and 4. Again for comparison a specimen of pure aluminium was also tested in the same environment; Fig. 10 shows the resulting plot.

4. Discussion

Despite the greater potential range achieved using lithium perchlorate solution, the potentiodynamic polarization plots obtained from the various test specimens (Figs 7–9) were very similar to one another. All the specimens were spontaneously passivated by the environment, hence no active to passive transition (which might have characterized the various samples) was recorded. There was, however, a small peak present on all of these plots, at approximately − 270 mV versus the reference electrode. This was absent from the corresponding plot obtained from the pure aluminium sample (Fig. 10).

The test samples were all based on the aluminium alloy 2014, which differed microstructurally from pure aluminium in that it contained a dispersion of second phase particles. These particles would have had their own distinct anodic polarization curve which would have been superimposed on that for the matrix phase when a potentiodynamic sweep was carried out. Thus it was likely that the peak observed on the experimental plots from all the test samples corresponded to an active/passive transition for the precipitate phase.

As can be seen from Table I, the rest potentials for the reinforced specimens differed both from one another and from the figure for unreinforced 2014 by tens of millivolts. These variations were very small compared with the large difference between E_{corr} for unreinforced 2014 and that for pure aluminium. Coupled with their randomness, this pointed to experimental scatter as opposed to a systematic variation in the results. The source of such scatter could have included incomplete stabilization of specimens before starting sweeps and/or slight pH variations in the distilled water used to make solutions.

Similar conclusions were drawn from the recorded pitting potentials. Again, there were small variations between the figures for the various 2014 specimens. However, these differences did not follow a trend and were small enough to be interpreted as scatter.

The small variations in the area of each hysteresis loop as seen in Figs 7 to 9 also suggested that the incorporation of the reinforcing materials into the host matrix did not have a significant influence on the susceptibilities of the metal matrix composites to undergo localized attack.

After each specimen had undergone a potentiodynamic sweep in the lithium perchlorate solution, there was clear visual evidence of the localized corrosion they had undergone. As shown in Plates 3 and 4, the pitting attack was not entirely random. The establishment of lines of pits was probably associated with microstructural variations resulting from the rolling process used to prepare the alloy samples, but this was not investigated further.

5. Conclusion

The addition of fine alumina or silicon carbide particles to give a reinforced composite of aluminium alloy 2014 does not appear to cause any dramatic deterioration in corrosion behaviour compared with unreinforced alloy. However, as these results were obtained by accelerated testing in a single electrolyte, they should be treated with caution. It is recommended that longer term exposure testing should be carried out in conditions typical of real service before the materials are used in potentially severe environments. It is possible that non-accelerated testing could reveal a tendency for corrosion to occur preferentially at the

matrix/reinforcement interface, which could lead to problems of stress corrosion cracking.

Acknowledgements

Thanks are due to Shell Research Ltd. for permission to publish this paper, to Mr T. S. Morgan for experimental assistance and to AEA Technology, Harwell for the supply of test specimens.

References

1. B. E. WILDE, *NACE Localised Corrosion* **3** (1971) 242.
2. C. A. FARINA, G. FAITA and F. OLIVANI, *Corrosion Science* **18** (1978) 465.

Received 7 January
and accepted 28 June 1994